AIMS Energy

http://www.aimspress.com/journal/energy

AIMS Energy, 6(4): 576–592.
DOI: 10.3934/energy.2018.4.576
Received: 02 June 2018
Accepted: 10 August 2018
Published: 15 August 2018

Research article

Design and performance analysis of quantitative feedback theory based automated robust controller : An application to uncertain autonomous wind power system

Gudimindla Hemachandra[1,*] **and Sharma K Manjunatha** [2]

[1] Research scholar, Department of Electrical and Electronics Engineering, National Institute of Technology Karnataka (NITK), Surathkal 575025

[2] Associate professor, Department of Electrical and Electronics Engineering, National Institute of Technology Karnataka (NITK), Surathkal 575025

* **Correspondence:** Email: sandhyahemachandra@gmail.com; Tel: +91 8618899095.

Abstract: Use of a robust controller for handling the operational uncertainties has become imperative in real time. This paper presents a modified fitness function based automated robust controller with the aid of quantitative feedback theory (QFT) using Genetic algorithm (GA). A controller exhibiting the desired decreasing modular plot and descending phase response is devised. The addition of arctangent function as one of the fitness function term is the proposed modification that facilitates in capturing the ideal controller characteristics. The proposed controller is applied to extract maximum power from a permanent magnet synchronous generator based autonomous wind power system. The step by step design guidelines for the automated QFT robust controller is deliberated in detail. The performance evaluation is carried out for step change and stochastically varying wind speed. Finally, benchmarking of the proposed controller against those available in the literature is accomplished through extensive simulations and it will be shown that the maximum power extraction along with least electromagnetic torque oscillations are achieved with the proposed fitness function based automated QFT controller.

Keywords: automatic loop shaping; genetic algorithm (GA); maximum power point tracking (MPPT); quantitative feedback theory (QFT); robust control; wind power system

Nomenclature

ρ	Air density (kg/m^3)
R_T	Blade radius (m)
λ	Tip-speed ratio
$C_T(\lambda)$	Torque coefficient
V_τ	Wind speed (m/s)
R	Rotor resistance (Ω)
R_s	Load resistance (Ω)
L_s	Load inductance (H)
p	Pole pair
L_d	d-axis rotor inductance (H)
L_q	q-axis rotor inductance (H)
i_d	d-axis rotor current (A)
i_q	q-axis rotor current (A)
J_h	Moment of inertia (kg-m^2)
ϕ_m	permanent magnet flux (Wb)
ω_h	Shaft speed (rad/s)
τ_{wt}	wind torque (N-m)
τ_{em}	electro-magnetic torque (N-m)

Abbreviations

2-DOF	Two degree of freedom
ALS	Automatic loop-shaping
AQFT	Automated quantitative feedback theory
AWPS	Autonomous wind power system
CAD	Computer aided design
CSD	Control system design
GA	Genetic Algorithm
HFG	High frequency gain
MAQFT	Modified automated Quantitative feedback theory
MMQFT	Multi-model Quantitative feedback theory
PFL	Partial feedback linearization
PMSG	Permanent magnet synchronous generator
QFT	Quantitative feedback theory

1. Introduction

Quantitative feedback theory (QFT) [1–4], is a robust control system design (CSD) approach which employs system output as an feedback variable to achieve the desired dynamic performance in presence of plant uncertainties and disturbances. In general, QFT is well applicable for handling uncertainty in frequency domain. Ever since its inception, QFT is applied to solve various real time CSD problems [2,3,5,6]. Although QFT was intially applied to different to various single input - single output (linear time variant, time invariant and nonlinear) systems, its extension to multiple input - multiple output

(linear and nonlinear) systems is presented in [5, 7, 8].

It is well known that for adequate implementation of QFT, system gain-phase loop-shaping is imperative and can be performed either manually or automatically. On this line many computer aided design (CAD) tools are developed to perform manual loop shaping like the pioneer Air Force Institute of Technology CAD tool [2, 9, 10], QFT control toolbox by European space agency author's group [11, 12], QFT MATLAB toolbox [7, 13] and Qsyn [14]. Despite its simplicity in design, the method primarily depends on the trial and error approach which indeed results in the system performance highly dependent on the designer. Further, the complexity increases profoundly for unstable and non-minimum phase uncertain systems in order to fulfil all the necessary performance specifications resulting in the need for automatic loop shaping (ALS) methods.

Concerning the attempts in developing the ALS methods, Gera and Horowitz proposed design of QFT robust controller based on iterative procedure to derive the shape of a nominal loop transfer function ($L(j\omega) = G(j\omega)P(j\omega)$) using Bode's gain phase integral [15]. However, the method requires a rational function approximation and straight line approximations leading to an underperforming CSD. Although Ballance and Gawthrop simplified the Bode's gain-phase integral iteration process, the possibility to address satisfactorily the specifications pertaining to noise rejection and stability is not well appreciable [16]. A method to approximate uncertain plant frequency responses using the nonlinear programming method is demonstrated in [17]. Approximation of templates based on the aforementioned method results in over bounding rectangles. To confront the issue of overbounding, linear programming based ALS using a series of linear approximations reported in [18] fails to define the QFT nonlinear bounds with linear inequalities. This drawback has been overcome by transforming the nonconvex closed loop bounds into linear inequalities by considering zeros alone as the optimization variables [19].

In addition, the authors, Garcia-sanz and Guillen [20], Garcia-sanz and Oses [21], and Garcia-sanz and Molins [22], have proposed the evolutionary and Genetic algorithm (GA) based ALS. Unlike the aforesaid methods, a phase independent controller is developed using the least square type algorithm [23]. Similarly, the application of particle swarm optimization, hybrid optimization (interval consistency and hull consistency), teaching learning-based optimization algorithm, flower pollination algorithm and convex concave optimization methods are presented in [8, 24–27] respectively. In spite of these many efforts, a simple design methodology to devise a controller with an overall satisfactory performance is still left unattended. With this motivation, an attempt to formulate a controller structure exhibiting the characteristics of descending modular trace within the close vicinity of the universal bound is addressed.

In this paper, a modified fitness function is formulated by considering the suitable cost function terms in order to accurately capture the desired descending modular trace close-packed to the universal bound. The minimization of the cost function is accomplished by the application of GA. The suitability and superiority of the proposed QFT based controller is demonstrated by applying it to an uncertain autonomous wind power system (AWPS). Numerical simulations are performed on MATLAB platform and results revealing the improved performance of the developed controller in comparison to the state-of-the-art methods are included. Finally, an exhaustive comparative analysis proving the proposed controller's improved performance with that of other well- established methods is carried out and the corresponding results are presented.

2. System description and QFT design procedure

A permanent magnet synchronous generator (PMSG) -based AWPS shown in Figure 1 is considered as the test system to demonstrate the applicability and suitability of the proposed QFT based robust controller under stochastic wind speeds [28–31]. Assuming that the other system components excluding those within the local control loop as highlighted in Figure 1 works as intended, with suitable assumptions, the chopper equivalent circuit is obtained [28]. Neglecting the dynamics of power electronic converters, dynamics pertaining to the aerodynamic model of wind turbine and PMSG are accounted. The aerodynamic torque is given as,

$$\tau_{wt} = \frac{1}{2}\rho\pi R_T^3 C_\tau(\lambda) V_\tau^2. \tag{1}$$

The dynamic model of PMSG with chopper equivalent variable resistance R_s in synchronous reference frame is given as,

$$\begin{aligned}
\frac{di_d}{dt} &= -\frac{(R+R_s)}{(L_d+L_s)} i_d + p\frac{(L_q-L_s)}{(L_d+L_s)} i_q \omega_h \\
\frac{di_q}{dt} &= -\frac{(R+R_s)}{(L_q+L_s)} i_q - p\frac{(L_d+L_s)}{(L_q+L_s)} i_d \omega_h + p\phi_m \\
\frac{d\omega_h}{dt} &= -\frac{1}{J_h}\tau_{wt} - \frac{\tau_{em}}{J_h} \\
\tau_{em} &= p[(L_d - L_q) i_d i_q - \phi_m i_q]
\end{aligned} \tag{2}$$

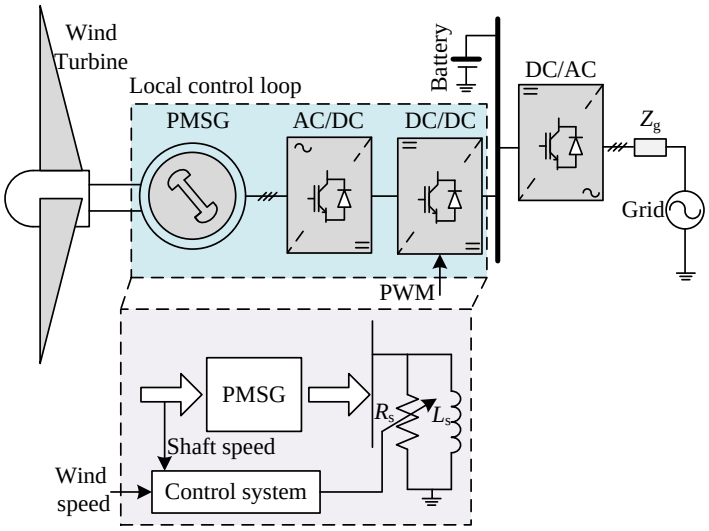

Figure 1. PMSG based autonomous wind turbine power system.

2.1. QFT Description

In real environment, the conventional control system fails to meet the necessary design specifications owing to its incapability to handle the uncertainties and disturbances that are inevitable

in any practical operating conditions. In order to attribute to these requirements, a highly robust CSD is essential. A two degree of freedom (2DOF) control structure shown in Figure 2 is used to design the robust controller and pre-filter in QFT framework [23]. Where $P(s)$ represents transfer function of the uncertain plant with $P \in \{p\}$, p representing the family of possible uncertain plants. The rationale behind the design of controller $G(s)$ and pre-filter $F(s)$ is to achieve robust stability and to meet the following performance specifications : Generally closed loop performance specifications are converted

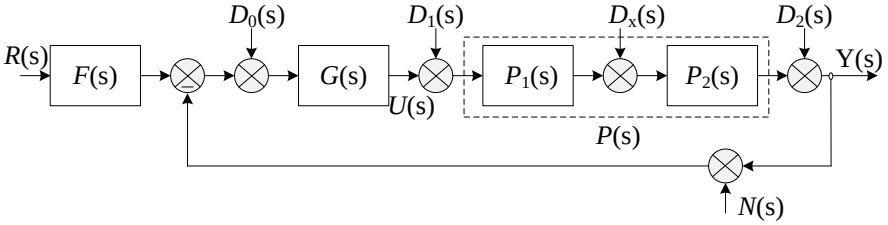

Figure 2. Two degree of freedom (2DOF) control system structure.

into frequency domain functions $\gamma_k(\omega)$ that are represented as transfer functions of robust stability and performance specifications, $|T_k(j\omega)|$ so that: $|T_k(j\omega)| \leq \gamma_k(\omega), k = 1...7$

2.1.1. Robust Stability

$$|T_1(j\omega))| = \left|\frac{U}{D_1}\right| = \left|\frac{Y}{D_0}\right| = \left|\frac{Y}{N}\right| = \left|\frac{L(j\omega))}{1 + L(j\omega))}\right| = \left|\frac{Y(j\omega)}{F(j\omega))R(j\omega)}\right| \leq \gamma_1(\omega) \tag{3}$$

2.1.2. Plant Output Disturbance

$$|T_2(j\omega))| = \left|\frac{Y}{D_2}\right| = \left|\frac{1}{1 + L(j\omega)}\right| \leq \gamma_2(\omega) \tag{4}$$

2.1.3. Plant Input Disturbance

$$|T_3(j\omega))| = \left|\frac{Y}{D_1}\right| = \left|\frac{P(j\omega)}{1 + L(j\omega))}\right| \leq \gamma_3(\omega)) \tag{5}$$

2.1.4. Robust Disturbance Rejection

$$|T_4(j\omega)| = \left|\frac{Y}{D_X}\right| = \left|\frac{P_2(j\omega)}{1 + L(j\omega)}\right| \leq \gamma_4(\omega) \tag{6}$$

2.1.5. Control Effort Attenuation

$$|T_5(j\omega)| = \left|\frac{U}{D_x}\right| = \left|\frac{G(j\omega)P_2(j\omega)}{1 + L(j\omega)}\right| \leq \gamma_5(\omega) \tag{7}$$

2.1.6. Control Effort Attenuation

$$|T_6(j\omega)| = \left|\frac{U}{N}\right| = \left|\frac{U}{D_2}\right| = \left|\frac{G(j\omega)}{1 + L(j\omega)}\right| = \left|\frac{U(j\omega)}{R(j\omega)F(j\omega)}\right| \leq \gamma_6(\omega) \tag{8}$$

2.1.7. Reference Tracking

$$\gamma_{7L}(\omega) \leq |T_7(j\omega)| = \left|\frac{Y}{R}\right| = \left|F(j\omega)\frac{L(j\omega)}{1 + L(j\omega)}\right| \leq \gamma_{7U}(\omega) \tag{9}$$

2.2. Step-by-Step QFT based Controller Design

The necessary procedure to be followed in the process of designing a QFT controller is comprehensively described below :

Step 1: Select the uncertain plant and define it's uncertainty range

Step 2: Establish the performance specifications

Step 3: Generate the template for an uncertain plant $P(s) \in p$, and select the frequency array $\omega_i, i = 1, ...l$. At each frequency obtain the variations of the plant parameters using the Nichols chart.

Step 4: Compute the QFT bounds by selecting the nominal plant such that the template points fulfils the performance specifications and are stable at every frequency for $\omega_i, i = 1, ...l$. Further compute the worst case bounds from the intersection of all the performance bounds at every frequency for $\omega_i, i = 1, ...l$.

Step 5: Perform the loop shaping $G(s)$ using the Nichols chart until the worst case bounds for every frequency are satisfied and a stable point for the closed loop nominal system is reached.

Step 6: Design the Pre-filters $F(s)$ using same principle of loop-shaping in order to enable the output to track the reference input.

2.3. High Frequency Gain

Reduction of high frequency noises at the sensor output and plant disturbances is desired to utilise the feedback benefits and is achieved by reducing high frequency gain (HFG) expressed as follows

$$HFG = \lim_{s\to\infty} s^r G(s) \tag{10}$$

where r represents the excess poles in G(s)

3. Automated QFT design

With this background the proposed design procedure of the automated QFT controller is presented in this Section. First, the problem statement formulation is discussed. Second, the modified fitness function evaluation is carried out.

3.1. Problem Statement

The critical design specifications such as reducing HFG there by maximizing the feedback benefits along with the minimization of cost of feedback are translated into a mathematical formulation given as,

$$G(x, j\omega) = K_G \frac{\prod_{i=1}^{n_z}(j\omega + z_i)}{\prod_{k=1}^{n_p}(j\omega + p_k)} \tag{11}$$

where $x = \left[K_G\,, p_1....p_{n_p}\,, z_1....z_{n_z}\right]$, K_G, p_k $((k = 1....n_p))$ and z_i $((i = 1...n_z))$ represents the real space parameters, gain, real poles and zeros respectively.

3.2. Fitness Function Formulation

In general, fitness function defined as combining an expression of constraints and objectives ideally defines quality of controller and its estimated behaviour. Hence it is very vital to formulate an effective fitness function and its coefficients which translates all the requisite CSD specifications into a mathematical expression. As a first step the controller excess gain-band width area on ω expressed as an integral form is given as,

$$A(\omega_1, \omega_2) = \int_{\omega_1}^{\omega_2} \ln|G(j\omega)|d\omega \tag{12}$$

The foregoing assumptions permit the computation of the definite integral of (12) in terms of $z_i, p_i, K_G, \omega_1 and \omega_2$ as follows (illustrated here for a proper controller,($n_z = n_p$):

$$A(\omega_1, \omega_2) = [\ln(K_G^2)(\omega_2 - \omega_1) + \sum_{i=1}^{n_z}\left(\omega_2 \ln\left[\frac{\omega_2^2 + z_i^2}{\omega_2^2 + p_i^2}\right] - \omega_1 \ln\left[\frac{\omega_1^2 + z_i^2}{\omega_1^2 + p_i^2}\right] + 2z_i\, tan^{-1}\Big(\frac{\omega_2}{z_i}\Big)\right.$$
$$\left. - 2p_i\, tan^{-1}\Big(\frac{\omega_2}{p_i}\Big) + 2z_i\, tan^{-1}\Big(\frac{\omega_1}{z_i}\Big) - 2p_i\, tan^{-1}\Big(\frac{\omega_1}{p_i}\Big)\right) \tag{13}$$

Finally, the controller gain-bandwidth area measure is used to form an augmented cost function. As an outcome, the formulated fitness function is given as,

$$J(x) = a_0\, k_G^2 + a_1 \sum_{i=1}^{n_z} \frac{(p_i - z_i)^4 + 1}{p_i z_i} + a_2\, A(\omega_1, \omega_2) + a_3\, V(x) + a_4 \sum_{i=1}^{n_z} tan^{-1}\left(\frac{p_i - z_i}{p_i z_i}\right) \tag{14}$$

In the above cost function, the first two terms corresponds to high frequency gain and lead ratios respectively while the third and fourth terms refers to constraint pertaining to the area and the penalty respectively. The third term in (14) facilitates the tight control of gain at any frequency of interest. Thus, helps in diminishing the over-design at low frequencies. Similarly, additional terms can be included in order to cater other frequency ranges as well.

In general the nominal loop transmission should satisfy the bounds of intersection and are described as a function q with lower and upper parts, q_l and q_u respectively, such that,

$$L_m q_u(\angle L_0(x, j\omega_i), \omega_i) \leq L_m L_0(x, j\omega_i) \qquad i \in I$$

$$L_m L_0(x, j\omega_i) \leq L_m q_l(\angle L_0(x, j\omega_i), \omega_i) \tag{15}$$

where $L_0 = GP_0$, I represents the frequency array points of interest, L_m indicates log10 magnitude, and P_0 is the nominal plant. Further, the lower and upper bound violation limits are given by,

$$\begin{aligned} \theta_{x,i} &= \angle L_0(x, \omega_i) \\ V_u(x, \omega_i) &= \max\{\log q_u(\theta_{x,i}, \omega_i) - \log L_0(x, \omega_i), 0\} \\ V_l(x, \omega_i) &= \max\{\log L_0(x, \omega_i) - \log q_l(\theta_{x,i}, \omega_i), 0\} \end{aligned} \tag{16}$$

$$V_\omega(x, \omega_i) = \begin{cases} \min\{V_u(x, \omega_i), V_l(x, \omega_i)\}, \\ \text{if } q_u(\theta_{x,i}, \omega_i) \geq q_l(\theta_{x,i}, \omega_i) \\ \max\{V_u(x, \omega_i), V_l(x, \omega_i)\}, \\ \text{otherwise} \end{cases} \tag{17}$$

Thus, the penalty function V(x) to penalise the unfeasible solutions that do not fulfil the performance specifications and assist in comprehending the degree of disparity of each bound at frequency ω_i is given by,

$$V(x) = \sum_{i \in I} V_\omega^2(x, \omega_i) \tag{18}$$

It is worth noting that despite the addition of the prominent and wide spread terms into the fitness function, the inclusion of the proposed fifth term greatly aids in obtaining the desired descending modular plot of the controller. The inherent characteristics of the proposed term results in impelling the locus of the closed loop transmission $L_0(s)$ as much as nearer to the Universal bound while exhibiting descending phase response. The so formulated fitness function helps in realising a well-nigh controller that performs well against real time system uncertainties and disturbances.

4. Application and results

The proposed QFT based robust controller and pre-filter design steps as applied to an PMSG-based AWPS is discussed in this Section. The transfer function model of PMSG based AWPS is represented as an uncertain system given by,

$$P(s) = \frac{k}{(1 + 2T\xi s + s^2T^2)} \tag{19}$$

where, the uncertainty of plant parameter is $6 \leq k \leq 20,\ 0.01 \leq T \leq 0.09,\ \xi = 0.8$. The nominal plant parameters are k = 20 and T = 0.09.

4.1. Template Generation

Templates are the pictorial representation of the uncertain plant's magnitude and phase response at fixed frequency. The sketch of the templates for the frequency vector ω = [1 5 10 20 30 40 50 100] rad/s shown in Figure 3.

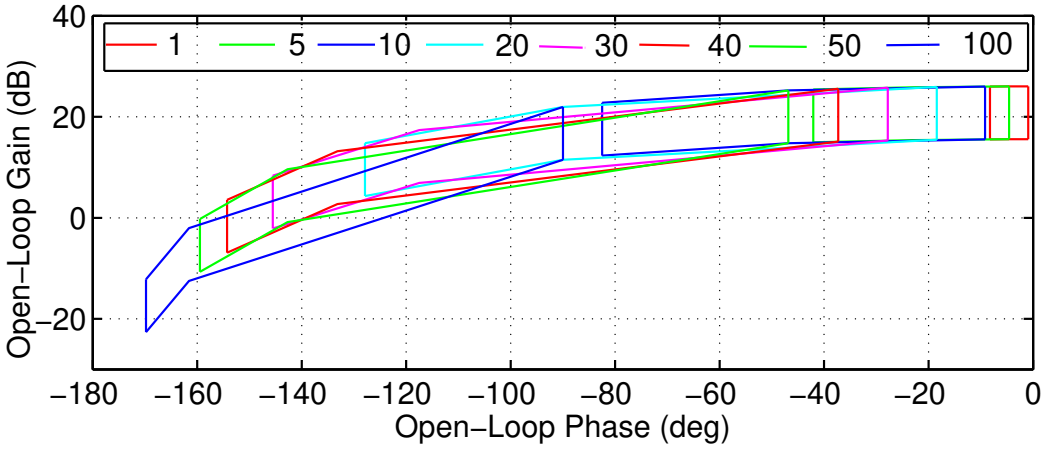

Figure 3. Template generation at different frequencies.

4.2. Computation of Bounds

The edge point templates are used to obtain QFT bounds. Stability margins and performance specifications are transformed to frequency domain in order to represent the QFT bounds in Nichols chart. The computation of QFT bounds is accomplished by considering the quadratic inequalities and the closed loop robust stability margins are given as,

$$\left|\frac{L(j\omega)}{1+L(j\omega)}\right| \leq \gamma_1 \quad \forall\ P \in \{p\} \tag{20}$$

In this case, $\gamma_1 = 1.2 = 1.6$ dB results in a gain margin and phase margin of 5.26483 dB and 49.2486^0 respectively.

The upper and lower reference tracking bounds for the considered AWPS are given by,

$$\begin{aligned} H_U(s) &= \frac{16.67s + 400}{s^2 + 36s + 400} \\ H_L(s) &= \frac{12000}{s^3 + 80s^2 + 1900s + 12000} \end{aligned} \tag{21}$$

Further, all the stability and tracking bounds are grouped to calculate the worst case possibilities and are pictorially depicted in Figure 4.

4.3. Loop Shaping

The existing and proposed ALS methodology based control structures formulated using GA are respectively given by,

$$G_1(s) = \frac{15.701(s + 42.29)(s + 38.43)(s + 10.42)}{(s + 354)(s + 134)(s + 0.01765)} \tag{22}$$

$$G_2(s) = \frac{5.7074(s + 53.06)(s + 23.58)(s + 13.63)}{(s + 125.1)(s + 109.6)(s + 0.07097)} \tag{23}$$

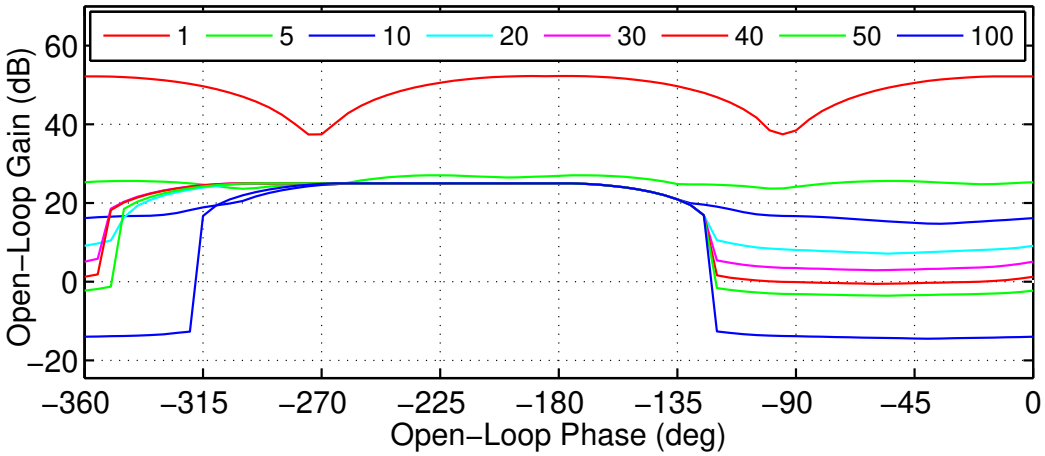

Figure 4. Intersection of Bounds.

It is evident from Figure 5 and Figure 6 that the open loop phase of $L_0(s)$ is closer to the universal bound for the proposed controller between the frequency 10 to 100 rad/s. In addition, performance comparison of existing and proposed controllers in terms of HFG and cost value is tabulated in Table 1. With the application of proposed controller, the HFG is reduced to a value of 63.65% as compared to the application of method described in [22]. Thus, the sensitivity of proposed controller to high frequency noise is minimum and requires reduced control effort. The reduced cost function value attests the lesser feedback cost requirement of the proposed controller.

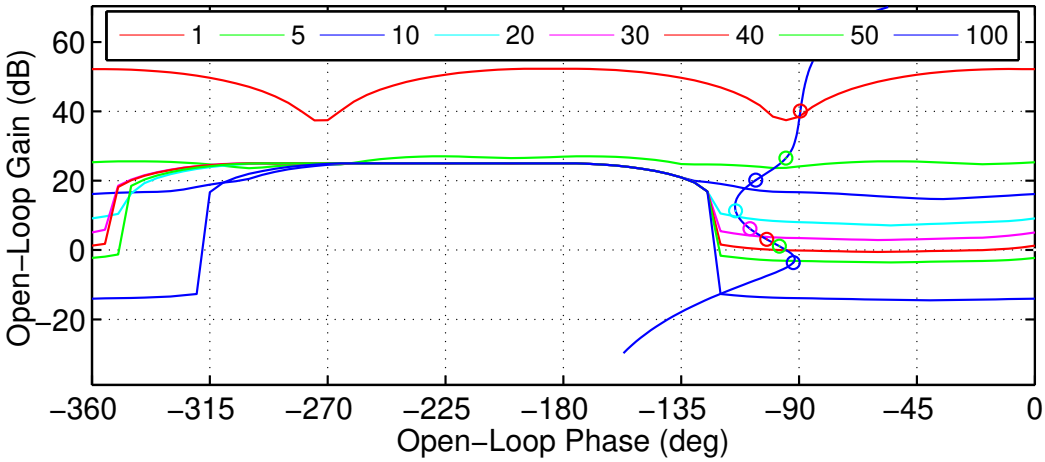

Figure 5. Loop-shaping with existing controller $G_1(s)$.

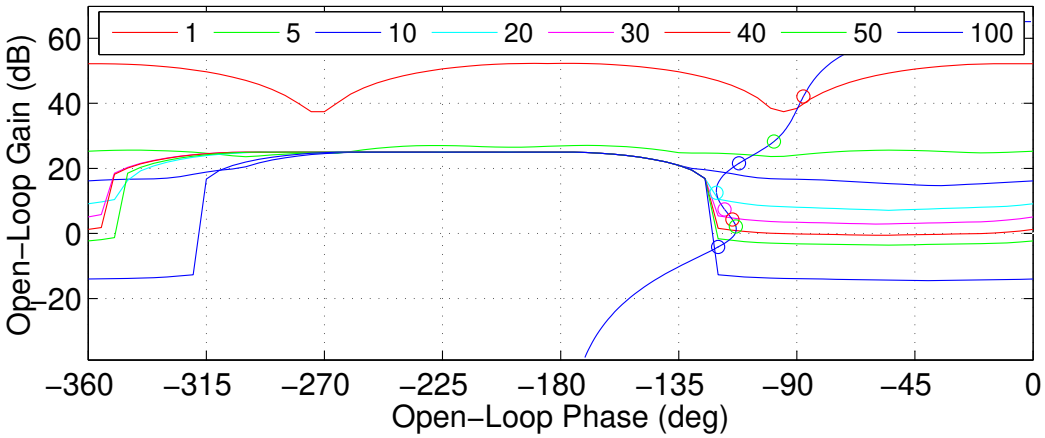

Figure 6. Loop-shaping with proposed controller $G_2(s)$.

Table 1. Performance Comparison of the Proposed Controller with [22].

Performance index	[22]	Proposed method
HFG	15.701	5.7074
J(x)	1.2286×10^5	1.0622×10^4

4.4. Pre-filter Design

The design of pre-filter is performed using the same procedure as that of loop-shaping and obtained transfer function is given as,

$$F(s) = \frac{1}{7.614 \times 10^{-6} s^3 + 0.00156 s^2 + 0.087 s + 1} \tag{24}$$

The corresponding block diagram representation of developed system with proposed subsystems is shown in Figure 7.

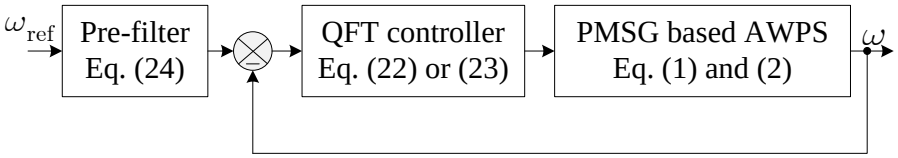

Figure 7. Automated QFT controller structure for PMSG based AWPS.

5. Performance evaluation

The maximum power tracking capability of the proposed controller under step change in wind speed and stochastic variation is tested and a comparative evaluation is performed against the following

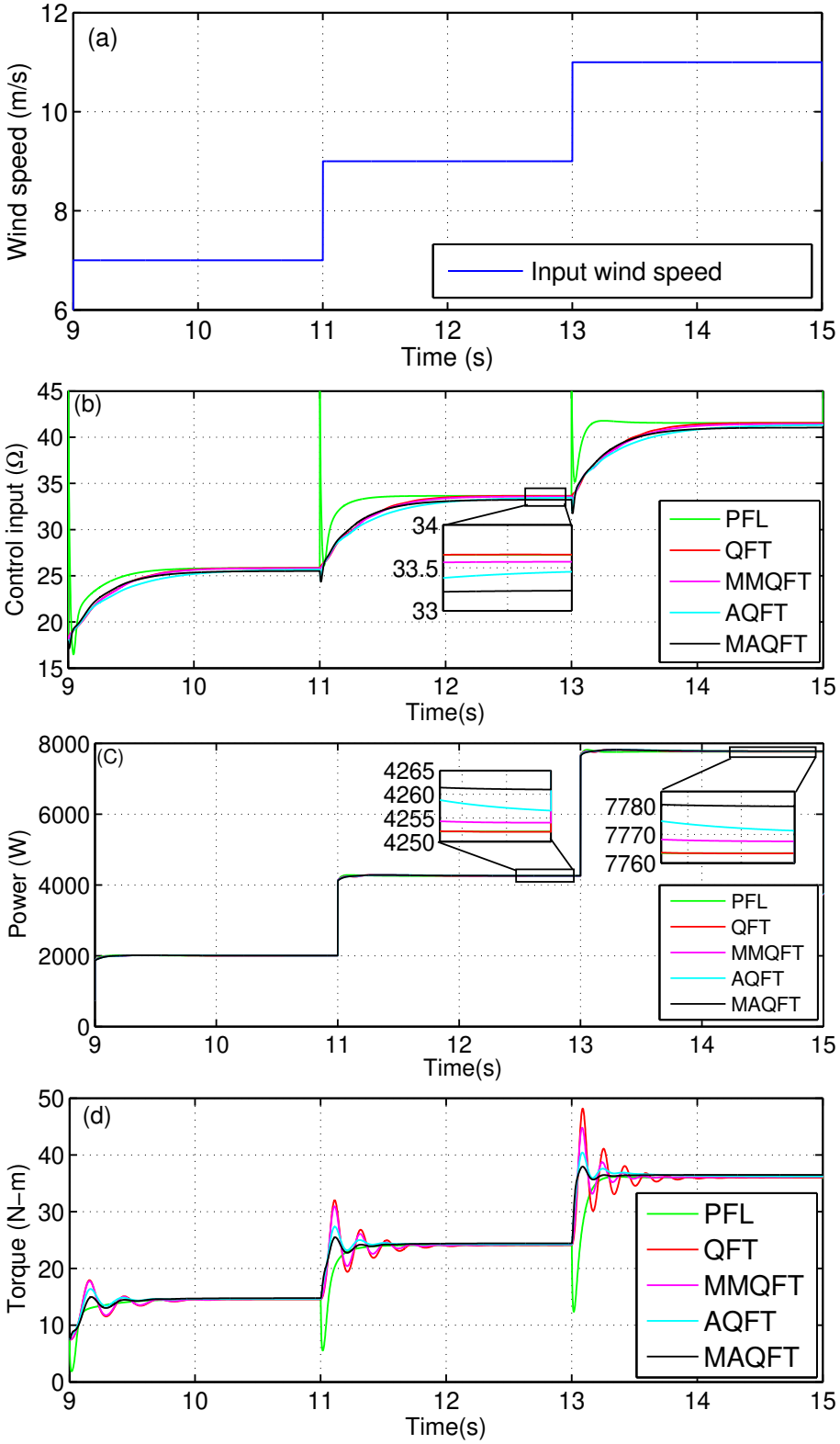

Figure 8. Step change in wind speed (a) Wind profile (b) Control input (c) Output power (d) Electro magnetic torque.

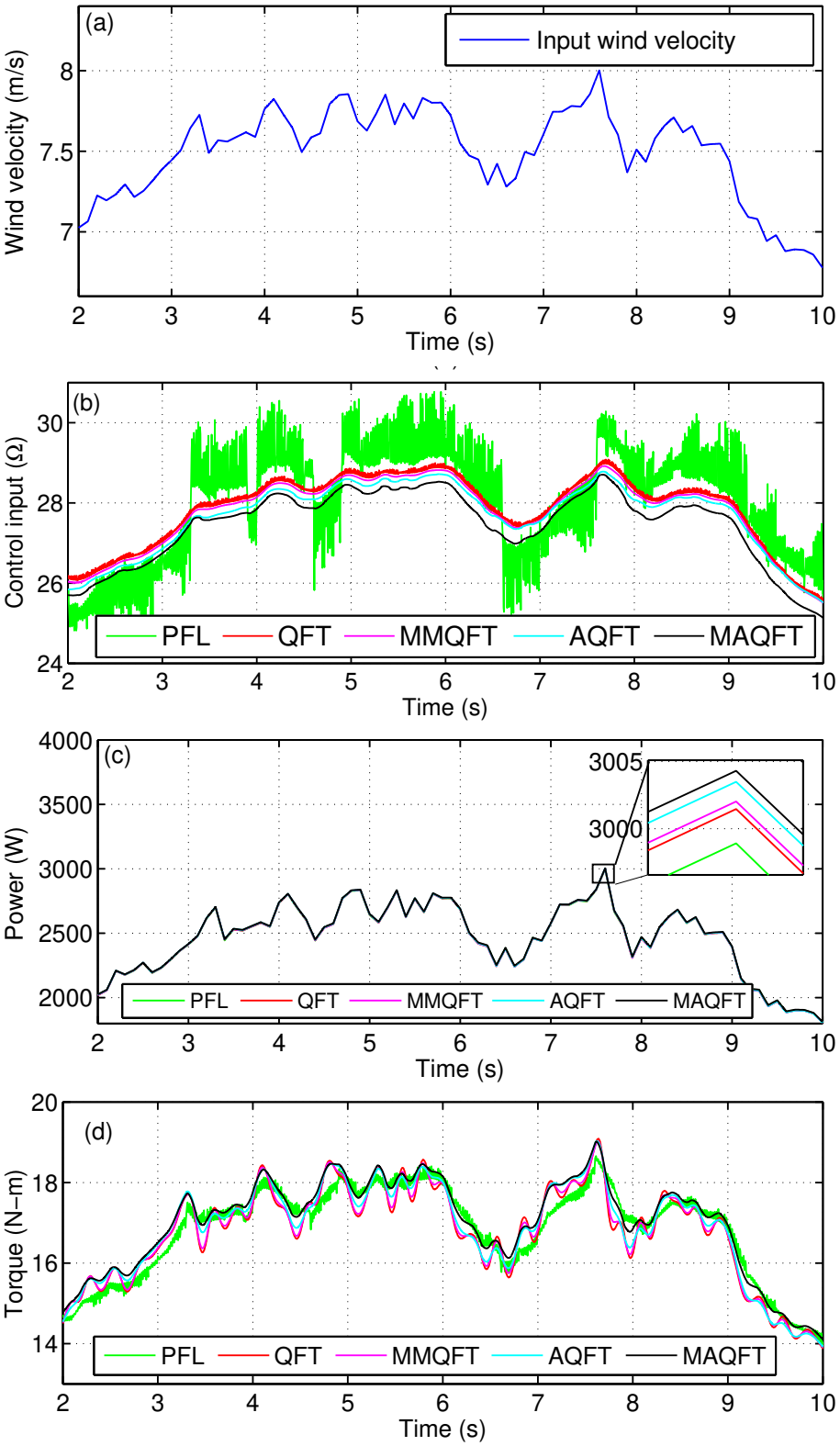

Figure 9. Stochastic wind speed (a) Wind profile (b) Control input (c) Output power (d) Electro magnetic torque.

methods: feedback linearization [29], QFT [28] , multi-model QFT [28], GA based automated QFT [22] through MATLAB simulations. The PMSG and wind turbine parameters employed for the simulation are shown in Table 2. The input wind velocity template depicts step variations at t = 11 s and 13 s is shown in Figure 8(a) . The corresponding variations in the control input, extracted power and the rotor torque are shown in Figure 8(b), 8(c) and 8(d) respectively. It is observed that the proposed controller requires the minimum control input while operating as desired. Also, it noteworthy that the proposed controller facilitates in extracting the maximum power corresponding to a given wind velocity in comparison to other well established techniques. It is highly desired to have a smooth torque variation

Table 2. System parameters.

Wind turbine parameters	PMSG parameters
R_T =2.5 m, ρ=1.25 kgm^{-3}	P=3, R=3.3 Ω, L_s=0.08 H, R_s=80 Ω
J_h=0.0552 $kg - m^2$	ϕ_m=0.4382 Wb, $L_q = L_d$=0.04156 H

Table 3. Performance comparison of controllers for step variation in wind speed.

Parameter	Wind profile	PFL	QFT	MMQFT	AQFT	MAQFT
Control input (Ω)	7 m/s	27	25.9	25.82	25.72	25.52
	7 ⇒ 9 m/s	33.65 + 33.63 %	33.65	33.55	33.45	33.24
	9 ⇒ 11 m/s	41.55 + 17.83 %	41.55	41.41	41.3	41
Electromagnetic torque (N-m)	7 m/s	14.7 ± 0.15 %	14.59	14.598	14.65	14.755
	7 ⇒ 9 m/s	24 - 75 %	24.1 + 32.78 %	24.16 + 28.31 %	24.23 + 13 %	24.42 + 4.42 %
	9 ⇒ 11 m/s	36 -65.67 %	36 + 34.03 %	36.1 + 23.96 %	36.3 + 11.57 %	36.5 + 4.11 %
Power extracted (W)	7 m/s	2000.54	2000.65	2001.02	2002.3	2004.75
	7 ⇒ 9 m/s	4252	4252	4254	4256.6	4261
	9 ⇒ 11 m/s	7763	7763	7767.6	7772.2	7780

$^{+}$ Overshoot;
$^{-}$ Decay;
$^{\pm}$ Oscillatory

owing to the associated mechanical structure. Among the other available methods, a smooth torque variation with an improved performance is witnessed with the application of the developed controller. Further the key observations proving the proposed controllers competency is enlisted in Table 3 .

Owing to the inherent variability in the wind power generation, a stochastic wind profile is consider as the second test case. The corresponding results are shown in Figure 9. It is evident from the result figures that the proposed controller outperforms the other available CSD methods from various control system perspectives.

6. Conclusion

This paper presented a modified fitness function based automated robust controller using GA in QFT framework to extract the maximum power from PMSG based AWPS. The prominent features of the proposed controller are as follows.

1. It absolutely exhibits the highly desired decreasing modular plot and descending phase response.
2. Addition of a simple arc tangent function helps in shifting the loop-shaping curve closer to the universal bound intern significantly reducing the gain at high frequencies.
3. The usage of GA leads to the effortless acquisition of the controller parameters.

The applicability and feasibility of the developed controller is verified through extensive simulations and the results attesting its improved performance against well established methods are presented.

Conflict of interest

All authors declare no conflicts of interest in this paper.

References

1. Horowitz IM (1963) *Synthesis of feedback systems*, New York: Academic Press.
2. Houpis CH, Rasmussen SJ, Garcia-Sanz M (2006) *Quantitative Feedback Theory. Fundamentals and Applications*, 2nd Edition, CRC Press.
3. Garcia-Sanz M, Houpis CH (2012) *Wind energy systems: control engineering design*, CRC Press.
4. Garcia-Sanz M (2017) *Robust Control Engineering: practical QFT solutions*, CRC Press.
5. Garcia-Sanz M, Eguinoa I, Barreras M, et al. (2008) Nondiagonal MIMO QFT controller design for Darwin-type spacecraft with large flimsy appendages. *J Dyn Syst-T ASME* 130: 011006.
6. Garcia-Sanz M, Molins C (2008) QFT Robust Control of a Vega-type Space Launcher. *IEEE Mediterranean Conference on Control and Automation* 16: 35–40.
7. Chait Y, Yaniv O (1993) Multi-Input/Single-Output computer-aided control design using the quantitative feedback theory. *Int J Robust Nonlin* 3: 47–54.
8. Jeyasenthil R, Purohit H, Nataraj PSV (2014) Automatic loop shaping in MIMO QFT using interval consistency based optimization technique. *IEEE 23rd International Symposium on Industrial Electronics (ISIE),* 75–80.
9. Houpis CH, Sating RR (1997) MIMO QFT CAD Package (Ver.3). *Int J Control* 7: 533–549.
10. Sating RR, Horowitz IM, Houpis CH (1993) Development of a MIMO QFT CAD Package (Ver. 2), Air Force Institute of Technology. *American Control Conference*.
11. Garcia-Sanz M, Mauch A, Philippe C (2009) QFT Control Toolbox: an Interactive Object-Oriented Matlab CAD tool for Quantitative Feedback Theory. *6th IFAC Symposium on Robust Control Design* 9: Haifa, Israel.
12. Garcia-Sanz M (2016) The QFT Control Toolbox (QFTCT) for Matlab,Version 9.45, Available from: `http://cesc.case.edu`.

13. Borghesani C, Chait Y, Yaniv O (2003) Quantitative Feedback Theory Toolbox v 2.0 - For use with MATLAB, Terasoft, 2003.

14. Gutman PO (1996) Qsyn - The Toolbox for Robust Control Systems Design for use with Matlab, User's Guide, Air Force Institute of Technology, *El-Op Electro-Optics Industries Ltd*, Rehovot, Israel.

15. Gera A, Horowitz IM (1992) Optimization of the loop transfer function. *Int J Control* 31: 389–398.

16. Balance DJ, Gawthrop PH (1991) Control systems design via a Quantitative Feedback Theory approach. *Proc of the IEE Conference Control*, Edinburgh, UK, 476–480.

17. Thompson DF, Nwokah ODI (1989) Stability and optimal design in quantitative feedback theory *Proc ASME WAM Conference*.

18. Bryant GF, Halikias GD (1995) Optimal loop-shaping for systems with large parameter uncertainty via linear programming. *Int J Control* 62: 557–568.

19. Chait Y, Chen Q, Hollot CV (1999) Automatic loop-shaping of QFT controllers via linear programming. *J Dyn Syst-T ASME* 121: 351–357.

20. Garcia-Sanz M, Guillen JC (2000) Automatic Loop-shaping of QFT Robust Controllers via Genetic Algorithms *3rd IFAC Symposium on Robust Control Design*, Prague, Czech Republic.

21. Garcia-Sanz M, Oses JA (2004) Evolutionary Algorithms for Automatic tuning of QFT Controllers. *Proceedings of the 23rd IASTED International Conference Modelling, Identification and Control*, Grindelwald, Switzerland.

22. Garcia-Sanz M, Molins C (2009) Automatic Loop-shaping of QFT Robust Controllers. *National Aerospace and Electronics Conference, NAECON'09*, Dayton, Ohio, USA.

23. Garcia-Sanz M, Molins C (2010) Automatic Loop Shaping of QFT Robust Controllers with Multi-objective Specifications via Nonlinear Quadratic Inequalities. *Proceedings of the IEEE Aerospace and Electronics Conference (NAECON)* 348–353.

24. Ali HI, Noor SBBM, Bashi SM, et al. (2012) Quantitative Feedback Theory control design using particle swarm optimization method. *T I Meas Control* 34: 463–476 .

25. Katal N, Narayan S (2016) QFT Based Robust Positioning Control of the PMSM Using Automatic Loop Shaping with Teaching Learning Optimization. *Model Simul Eng* 2016: 1–18.

26. Katal N, Narayan S (2016) Optimal QFT controller and pre-filter for buck converter using flower pollination algorithm. *IEEE International Conference on Power Electronics, Intelligent Control and Energy Systems (ICPEICES),* 1–6 .

27. Mercader P, Astrom KJ, Banos A, et al. (2017) Robust PID Design Based on QFT and Convex-Concave Optimization. *IEEE T Contr Syst T* 25: 441–452.

28. Cutululis NA, Ceanga E, Hansen AD, et al. (2006) Robust multi-model control of an autonomous wind power system. *Wind Energy* 9: 399–419.

29. Huang Y, Li H, Li G, et al. (2014) The Largest Wind Energy Capture Based on Feedback Linearization Control. *Unifying Electrical Engineering and Electronics Engineering, Springer* 238: 1011–1018.

30. Taraft S, Rekioua D, Aouzellag D, et al. (2015) A proposed strategy for power optimization of a wind energy conversion system connected to the grid. *Energ Convers Manage* 101: 489–502.

31. Gupta RA, Singh B, Jain BB (2015) Wind energy conversion system using PMSG. *International Conference on Recent Developments in Control, Automation and Power Engineering (RDCAPE)*, 199–203.

AIMS Press